

## MIT Open Access Articles

*Electroactive Anion Receptor with High Affinity for Arsenate*

The MIT Faculty has made this article openly available. **Please share** how this access benefits you. Your story matters.

**Citation:** Etkind, Samuel I. et al. "Electroactive Anion Receptor with High Affinity for Arsenate." *Journal of Organic Chemistry* 85, 15 (July 2020): 10050–10061 © 2020 American Chemical Society

**As Published:** <http://dx.doi.org/10.1021/acs.joc.0c01206>

**Publisher:** American Chemical Society (ACS)

**Persistent URL:** <https://hdl.handle.net/1721.1/128150>

**Version:** Author's final manuscript: final author's manuscript post peer review, without publisher's formatting or copy editing

**Terms of use:** Creative Commons Attribution-Noncommercial-Share Alike



# An Electroactive Anion Receptor with High Affinity for Arsenate

Samuel I. Etkind<sup>†</sup>, Douglas A. Vander Griend<sup>‡</sup>, Timothy M. Swager<sup>†\*</sup>

<sup>†</sup> Department of Chemistry, Massachusetts Institute of Technology, Cambridge, MA, 02139, USA.

<sup>‡</sup> Department of Chemistry and Biochemistry, Calvin University, Grand Rapids, Michigan, 49546, USA.

**KEYWORDS** (*Word Style "BG\_Keywords"*). *If you are submitting your paper to a journal that requires keywords, provide significant keywords to aid the reader in literature retrieval.*

**ABSTRACT:** Herein we present the synthesis and characterization of a macrocyclic polyamide cage that incorporates redox-active 1,4-dithiin units. UV/Vis titration experiments with eight anions in acetonitrile revealed high affinity for H<sub>2</sub>AsO<sub>4</sub><sup>-</sup> (logβ<sub>2</sub> = 10.4<sup>+0.4</sup><sub>-0.4</sub>) and HCO<sub>3</sub><sup>-</sup> (logβ<sub>2</sub> = 8.3<sup>+0.3</sup><sub>-0.4</sub>) over other common anionic guests, such as Cl<sup>-</sup> (logK<sub>1:1</sub> = 3.20<sup>+0.03</sup><sub>-0.02</sub>), HSO<sub>4</sub><sup>-</sup> (logK<sub>1:1</sub> = 3.57<sup>+0.02</sup><sub>-0.03</sub>) and H<sub>2</sub>PO<sub>4</sub><sup>-</sup> (logK<sub>1:1</sub> = 4.24<sup>+0.05</sup><sub>-0.04</sub>), by the selective formation of HG<sub>2</sub> complexes. The recognition of arsenate over phosphate is rare among both proteins and synthetic receptors, and exploiting the difference in binding stoichiometry represents an underexplored avenue towards developing receptors that can differentiate between the two anions. Additional analysis by <sup>1</sup>H-NMR in 1:3 CD<sub>2</sub>Cl<sub>2</sub>:MeCN-*d*<sub>3</sub> found strong dependence of anion binding stoichiometry with the solvent employed. Finally, titration experiments with cyclic voltammetry provided varying and complex responses for each anion tested, though reaction between the anion and receptors was observed in most cases. These results implicate 1,4-dithiins as interesting recognition moieties in the construction of supramolecular receptors.

## Introduction

Simple anions can often act as potent environmental pollutants. For examples, nitrate and phosphate leached from fertilizers can lead to algae blooms, depriving aquatic ecosystems of oxygen needed to sustain animal life.<sup>1</sup> Increasing levels of atmospheric CO<sub>2</sub> levels is coupled with an increase in oceanic bicarbonate concentration and therefore ocean acidity, resulting in the degradation of CaCO<sub>3</sub>, a protective layer for many organisms.<sup>2</sup> Millions in Bangladesh are at risk of arsenic poisoning, which could be mitigated by the environmental monitoring of arsenate levels.<sup>3</sup> Typically, the accurate quantification and detection of anions at environmentally relevant concentrations requires the use of costly analytical methods, such as HPLC and ICP-MS.<sup>4-7</sup> These methods, however, could be potentially supplanted by cost-effective techniques that use supramolecular receptors to aid in the detection of anionic species.

To apply anion receptors to the detection of anions in complex mixtures, researchers utilize a variety of methods, such as change in fluorescence,<sup>8-11</sup> absorbance (i.e. colorimetric sensors),<sup>12-14</sup> or NMR resonance<sup>15-19</sup> in the presence of guests. More recently, there have been efforts by a number of groups to employ electrochemical methodology towards the detection of anions via chemiresistive,<sup>20</sup> potentiometric,<sup>21,22</sup> capacitive,<sup>23</sup> or redox-based sensing,<sup>24</sup> due to their potential application in the development of cost-effective devices. We were particularly drawn to the development of redox-active receptors, as the effect of transiently creating cationic species has the potential to effectively bind anions in competitive media, such as water.<sup>25</sup>

Electroactive anion receptors have been well described.<sup>25</sup> Most designs involve appending a redox transducer, most commonly ferrocene,<sup>26-28</sup> to a known anion receptor; however, **Scheme 1. Preparation of Receptor 3.**

other strategies have been employed, such as the use of electroactive ureas<sup>29</sup> and mixed valence systems.<sup>30</sup> The change in reduction potential upon introduction of an anionic guest is proposed to proceed via a variety of mechanisms, including through-space interactions between the redox-active moiety and anion as well conformational changes of the redox transducer upon anion complexation, which result in the guest binding to the oxidized host with a greater affinity than the non-oxidized host.<sup>31</sup> The reduction potential of the host-guest complexes may differ depending on the included guest. Additionally, the observation of ‘two-wave’ behavior, in which the host and guest are in slow equilibria, could potentially be useful in differentiating between multiple anionic species.<sup>25</sup>

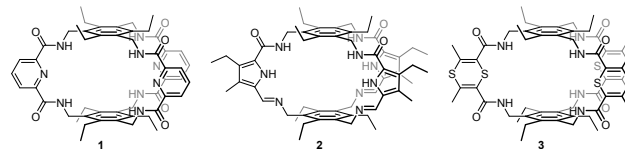
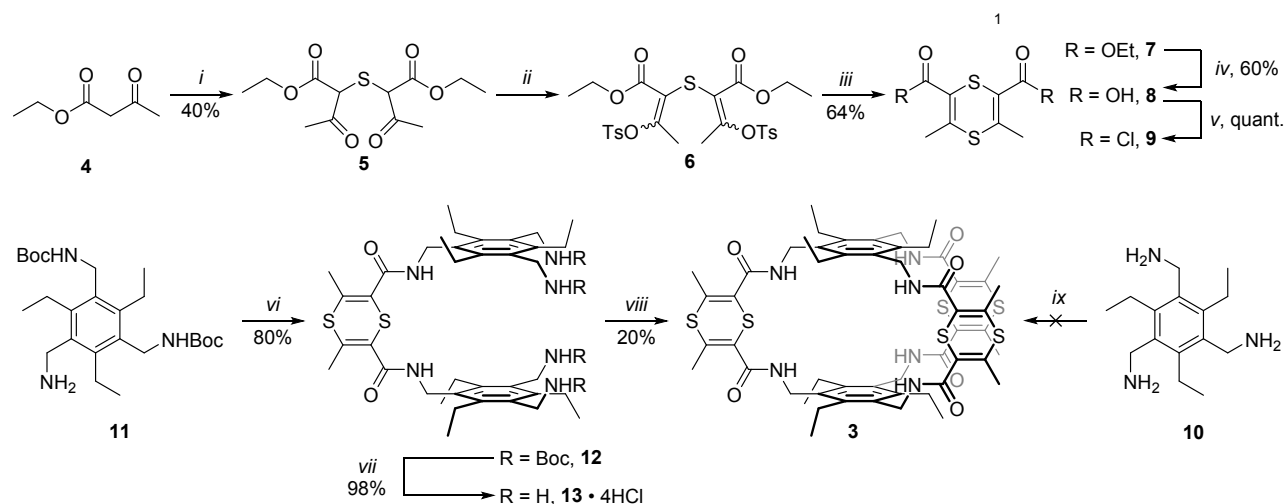


**Figure 1.** Previously reported polyamide cages **1** and **2** and new cage **3**.

We hypothesized that the modification of an existing anion receptor with a carefully chosen redox-transducer that is in close proximity to the binding site could give large shifts in the reduction potential of the host-guest complex upon oxidation. The modification of known supramolecular receptor scaffolds, such as in the introduction of halogen bonding,<sup>32,33</sup> altering distal functionalities to bias host-host<sup>34</sup> or host-guest interactions,<sup>35</sup> or systematically altering the size and electronic biases of the binding site<sup>36-41</sup> has been demonstrated to be an effective approach towards designing receptors with high affinity towards various anions, in addition to giving novel



Reagents and conditions: *i*)  $S_2Cl_2$ , hexanes, 35 °C, 1 h, 40 % *ii*) NaH, THF, 0 °C;  $Ts_2O$ , 0 °C to rt, 4 h *iii*)  $Na_2S \cdot 9H_2O$ , EtOH, 1.5 h, 64% (2 steps) *iv*) KOH, EtOH, 50 °C, 2 h, 60% *v*)  $(COCl)_2$ , cat. DMF,  $CH_2Cl_2$ , 2 h, quant. *vi*) **9**,  $Et_3N$ ,  $CH_2Cl_2$ , 0 °C to rt, 16 h, 80% *vii*) HCl, dioxane, 1 h, 98% *viii*) **9** (slow addition),  $Et_3N$ ,  $CHCl_3$  (1.5 mM), 20 h, 45 °C, 20% *ix*) **9** (slow addition), various conditions, <5%.

insights in structure-property relationships. Additionally, we recognized 1,4-dithiin, a sulfur rich heterocycle that exhibits a well-behaved single electron oxidation that is coupled with a geometric change from bent to planar, as largely overlooked in supramolecular scaffolds.<sup>42</sup> Herein, we present our work on the incorporation of 1,4-dithiin moieties into Receptor **1** to form Receptor **3**, which was previously reported as a nitrate-selective receptor by Anslyn and coworkers (Figure 1).<sup>43</sup> Notably, Kim, Sessler and coworkers have demonstrated the effectiveness of systematic alterations to Anslyn's Receptor **1** in the development of pyrrole and imine containing Receptor **2**, which shows a stronger preference for tetrahedral anions via the incorporation of hydrogen bond accepting moieties.<sup>44</sup>

Placement of the 1,4-dithiin units adjacent to the binding site could give large electrochemical responses via both through-space interactions between the anionic guest and redox transducer and the conformational change of the redox-active moiety upon oxidation. We also postulated that the formation of a tricationic cavity upon oxidation may form sufficiently strong interactions with anions to overcome their large solvation energy in highly polar media.

## Results and Discussion

**Synthesis.** The preparation of Receptor **3** was carried out according to Scheme 1 (See Supporting Information 1.1 for preparation of starting materials). The treatment of ethyl acetoacetate (**4**) with disulfur dichloride in hexane furnishes thioether **5**.<sup>45</sup> Initial efforts involved direct conversion of **5** to dithiin **7** via a variety of thionation reagents, such as Lawesson's reagent, Curphey's reagent, and  $P_4S_{10}$ , but such attempts resulted in the formation of complex mixtures. Instead, **5** can be treated with sodium hydride and  $Ts_2O$  to yield vinyl tosylate **6** as a mixture of isomers. Treatment of the crude mixture with sodium sulfide gives dithiin **7**, which can then be hydrolyzed to give diacid **8**. This serves as a highly efficient methodology to form 1,4-dithiin rings, the synthetic literature

**Table 1. Stability Constants of 3 with Various Anions**

Anion	$\log K_{1:1}$	$\log K_{1:2}$	$\log \beta_2$	$\Delta G_{K_{1:1}}$	$\Delta G_{K_{1:2}}$	$\Delta G_{\beta_2}$	$\alpha^a$
-------	----------------	----------------	----------------	----------------------	----------------------	----------------------	------------

of which has been limited in scope. In addition, gram scale synthesis of diacid **8** was enabled via this synthetic route. Conversion to diacyl chloride **9** can be accomplished by oxalyl chloride under standard conditions.

We initially attempted the direct cyclization of acyl chloride **9** with triamine **10** to form Receptor **3**; however, this resulted primarily in the formation of oligomeric species. A more robust approach involves molecule **13**, which can be synthesized starting with the preparation of protected amine **11**, followed by coupling with acyl chloride **9** to form **12** and deprotection under acidic conditions.<sup>46</sup> Use of HCl in dioxane as a deprotecting agent was crucial as the use of trifluoroacetic acid resulted in the formation of unidentified side products. Slow addition of acyl chloride **9** to **13** in a dilute solution of chloroform with gentle heating provided Receptor **3** in 20% yield (Supporting Information 4). The structure was confirmed by NMR, HRMS, and X-ray crystallography (Supporting Information 6). Notably, the X-ray structure shows all amide N-H bonds oriented towards the cavity of the receptor, potentially pre-organizing the scaffold towards interacting with anions (Figure 2).

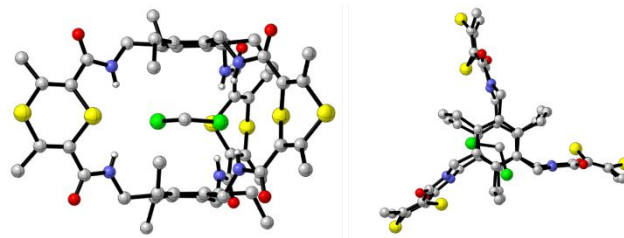


**Figure 2.** Side (left) and top (right) view of the crystal structure of Receptor **3** with  $CH_2Cl_2$  as a solvate. C-H hydrogens are omitted for clarity

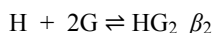
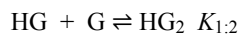
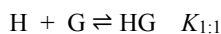
**Binding Characterization.** Association constants of Receptor **3** in acetonitrile with various tetrabutylammonium or

1	H <sub>2</sub> AsO <sub>4</sub> <sup>-</sup>	5.0 <sup>+0.4</sup> <sub>-0.3</sub>	5.4 <sup>+0.2</sup> <sub>-0.2</sub>	10.4 <sup>+0.4</sup> <sub>-0.4</sub>	-27 <sup>+2</sup> <sub>-2</sub>	-29 <sup>+1</sup> <sub>-1</sub>	-57 <sup>+2</sup> <sub>-2</sub>	9
2	HCO <sub>3</sub> <sup>-b</sup>	4.76 <sup>+0.06</sup> <sub>-0.30</sub>	3.53 <sup>+0.19</sup> <sub>-0.05</sub>	8.3 <sup>+0.3</sup> <sub>-0.4</sub>	-26.1 <sup>+1.7</sup> <sub>-0.3</sub>	-19.4 <sup>+0.3</sup> <sub>-1.1</sub>	-45 <sup>+2</sup> <sub>-2</sub>	0.25
3	OAc <sup>-</sup>	5.22 <sup>+0.05</sup> <sub>-0.10</sub>	- <sup>c</sup>	- <sup>c</sup>	-28.7 <sup>+0.5</sup> <sub>-0.3</sub>	- <sup>c</sup>	- <sup>c</sup>	- <sup>c</sup>
4	H <sub>2</sub> PO <sub>4</sub> <sup>-</sup>	4.24 <sup>+0.05</sup> <sub>-0.04</sub>	- <sup>c</sup>	- <sup>c</sup>	-23.3 <sup>+0.2</sup> <sub>-0.3</sub>	- <sup>c</sup>	- <sup>c</sup>	- <sup>c</sup>
5	CN <sup>-</sup>	3.69 <sup>+0.04</sup> <sub>-0.03</sub>	- <sup>c</sup>	- <sup>c</sup>	-20.3 <sup>+0.2</sup> <sub>-0.2</sub>	- <sup>c</sup>	- <sup>c</sup>	- <sup>c</sup>
6	HSO <sub>4</sub> <sup>-</sup>	3.57 <sup>+0.02</sup> <sub>-0.03</sub>	- <sup>c</sup>	- <sup>c</sup>	-19.6 <sup>+0.2</sup> <sub>-0.1</sub>	- <sup>c</sup>	- <sup>c</sup>	- <sup>c</sup>
7	NO <sub>3</sub> <sup>-</sup>	3.47 <sup>+0.03</sup> <sub>-0.03</sub>	- <sup>c</sup>	- <sup>c</sup>	-19.1 <sup>+0.2</sup> <sub>-0.2</sub>	- <sup>c</sup>	- <sup>c</sup>	- <sup>c</sup>
8	Cl <sup>-</sup>	3.20 <sup>+0.03</sup> <sub>-0.02</sub>	- <sup>c</sup>	- <sup>c</sup>	-17.6 <sup>+0.1</sup> <sub>-0.1</sub>	- <sup>c</sup>	- <sup>c</sup>	- <sup>c</sup>

11 Titrations were performed at 20 °C in MeCN using the tetrabutylammonium salt of each anion. UV/Vis data fitting was performed using  
 12 SIVVU. Errors are given from at least three experiments with asymmetric errors at 95% confidence intervals. <sup>a</sup>Interaction parameter, defined  
 13 as  $\alpha = \frac{4K_{1,2}}{K_{1,1}}$  <sup>b</sup>Tetraethylammonium bicarbonate was employed. <sup>c</sup>Not applicable.

15 tetraethylammonium salts were determined via UV/Vis  
 16 titrations, using SIVVU for data analysis (Table 1, Supporting  
 17 Information 2).<sup>47,48</sup> We chose a list of environmentally and  
 18 biologically relevant monoanionic guests to probe the binding  
 19 behavior of Receptor **3**. Asymmetric errors on the binding  
 20 constant terms were calculated by bootstrapping each dataset  
 21 column-wise 1000 times.<sup>49</sup> The errors of at least three separate  
 22 titrations were then combined according to Model 2 of Barlow's  
 23 paper and reported as 95% confidence intervals.<sup>50</sup> The  
 24 absorbance of all species, including the host, guest, and  
 25 complexes thereof, were refined as part of our data analysis. As  
 26 a result of the low concentration used for titration experiments  
 27 (<35 μM) and the polar solvent employed, ion-pairing  
 28 interactions were ignored.<sup>51</sup> Binding stoichiometries were  
 29 assessed by applying various binding models in the formation  
 30 of HG and HG<sub>2</sub> species to each experiment and selecting the  
 31 binding stoichiometry that gave the lowest error, as is currently  
 32 considered best practices.<sup>52,53</sup> Additionally, the simpler binding  
 33 model was selected in situations where multiple models gave  
 34 similar error. In the cases of select anions, such as H<sub>2</sub>AsO<sub>4</sub><sup>-</sup>,  
 35 H<sub>2</sub>PO<sub>4</sub><sup>-</sup>, HSO<sub>4</sub><sup>-</sup>, and NO<sub>3</sub><sup>-</sup>, titrations were performed at least  
 36 two concentrations between 5 μM and 35 μM to give further  
 support to the assigned binding stoichiometry and determined  
 association constant.

37 Cl<sup>-</sup> was bound with low affinity, a useful feature given its  
 38 ubiquity in environmental and biological settings. NO<sub>3</sub><sup>-</sup>, HSO<sub>4</sub><sup>-</sup>,  
 39 and CN<sup>-</sup> were bound with moderate affinity, followed by  
 40 H<sub>2</sub>PO<sub>4</sub><sup>-</sup> and OAc<sup>-</sup> with stronger binding affinity. Additionally,  
 41 when measuring the stability constants of Receptor **3** with  
 42 HCO<sub>3</sub><sup>-</sup>, binding isotherms were produced that could not be  
 43 accurately fit to a 1:1 binding model, and with H<sub>2</sub>AsO<sub>4</sub><sup>-</sup>,  
 44 application of a 1:1 binding model provided fits that were  
 45 associated with higher error than our other anion binding  
 46 experiments. Instead, it was found that the binding of H<sub>2</sub>AsO<sub>4</sub><sup>-</sup>  
 47 and HCO<sub>3</sub><sup>-</sup> could be more accurately fit with a 1:2 host:guest  
 binding mode in accordance with the following equations:



51  
 52 From the  $K_{1,1}$  and  $K_{1,2}$  values, the binding cooperativity can  
 53 be assessed by calculation of the interactivity parameter  $\alpha$

(Table 1).<sup>53</sup> Interestingly, while HCO<sub>3</sub><sup>-</sup> demonstrates negative  
 cooperativity ( $\alpha = 0.25$ ), H<sub>2</sub>AsO<sub>4</sub><sup>-</sup> demonstrates positive  
 cooperativity ( $\alpha = 9$ ), indicating that the binding of one anionic  
 species makes binding of the second more favorable. Such  
 binding stoichiometry may be indicative of the formation of  
 anti-electrostatic hydrogen bonding;<sup>54–58</sup> however, we have  
 been able to obtain neither solution nor solid state evidence for  
 the exact binding mode of these two anions.

We were especially surprised to discover the 1:2 binding  
 behavior in the case of H<sub>2</sub>AsO<sub>4</sub><sup>-</sup> does not hold for H<sub>2</sub>PO<sub>4</sub><sup>-</sup>, given  
 their similar sizes and properties.<sup>59</sup> We closely scrutinized this  
 behavior by subjecting several arsenate and phosphate titrations  
 to both 1:1 and 1:2 binding models in order to assess the best  
 fit. The absorbance and accompanying fits from 1:1 and 1:2  
 binding models at 292 nm is shown in Figure 3. We found  
 analysis of the residuals to be particularly useful in  
 determination of the binding stoichiometry, and such analysis  
 has been demonstrated to be significantly more informative and  
 robust than Job's plot analysis.<sup>52,60</sup> As shown in Figure 3a-b, the  
 application of a 1:1 binding model for H<sub>2</sub>AsO<sub>4</sub><sup>-</sup> results in  
 residuals that trace a sinusoidal curve, which has been  
 demonstrated to be indicative of an additional binding event.<sup>60</sup>  
 Additionally, a global fit of this experiment results in extinction  
 coefficients for the HG complex of 0 at certain wavelengths, a  
 non-realistic value, and large absorbance of the guest, an artifact  
 not observed in the absence of the host (Figure S81). Removing  
 guest absorbance from the binding model does not improve the  
 resulting fit. Application of a 1:2 binding model, instead,  
 provides significantly reduced residuals, and realistic extinction  
 coefficients for all species involved (H, G, HG, and HG<sub>2</sub>)  
 (Figure S83). Application of the same process to titration  
 experiments with H<sub>2</sub>PO<sub>4</sub><sup>-</sup> provides similar residuals for both the  
 1:1 and 1:2 binding models, which is indicative that a 1:2  
 binding model is not necessary to account for change in  
 absorbance (Figure 3c-d). Thus, evidence from UV/Vis titration  
 experiments indicate that phosphate and arsenate undergo  
 different binding events with Receptor **3** in acetonitrile (See  
 Supporting Information 2 for global fits of all titrations and 3D  
 plots of residuals). Indeed, strong selectivity between arsenate  
 and phosphate is rare in both proteins and synthetic receptors,  
 and only a few reports are present in the literature.<sup>39,61–63</sup>

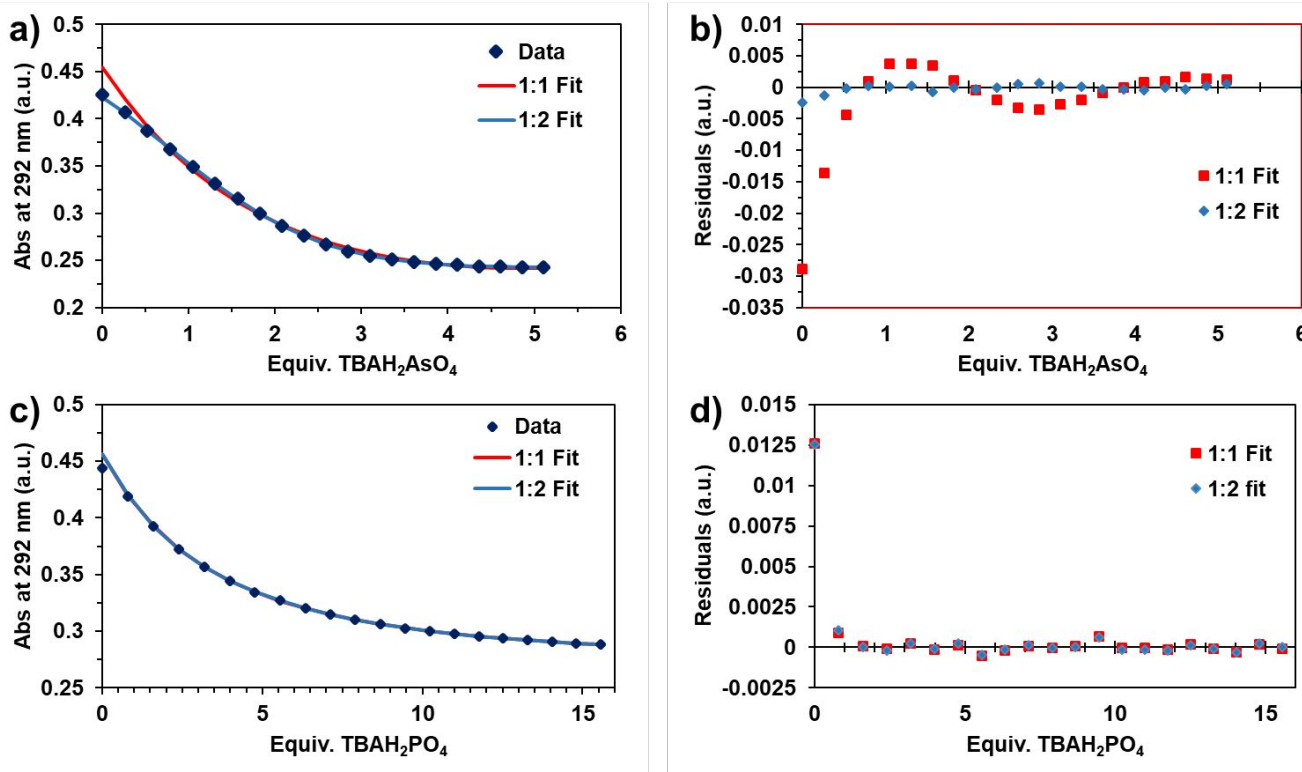
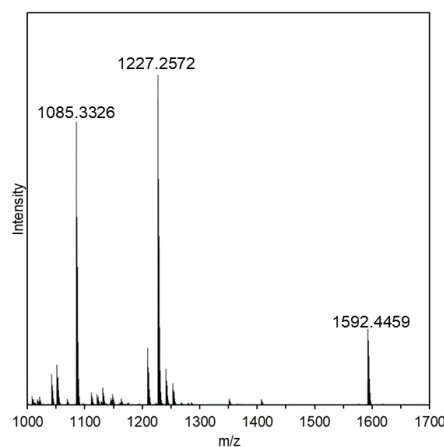


**Figure 3.** Comparison of 1:1 and 1:2 fits of Receptor **3** at a) 28.7  $\mu\text{M}$  after the addition of 5.08 equivalents of  $\text{TBAH}_2\text{AsO}_4$  with b) the resulting residuals from application of 1:1 and 1:2 binding models and c) 30.0  $\mu\text{M}$  after the addition of 15.5 equivalents of  $\text{TBAH}_2\text{PO}_4$  with d) the resulting residuals from application of 1:1 and 1:2 binding models. Absorbance data from 275–500 nm was used to determine the association constant and absorbance of all species in solution. Full binding models for these experiments are available in the Supporting Information in Figures S81–84 and Figure S65–68 for  $\text{TBAH}_2\text{AsO}_4$  and  $\text{TBAH}_2\text{PO}_4$ , respectively.

We sought to further probe the difference in binding behavior between  $\text{H}_2\text{AsO}_4^-$  and  $\text{H}_2\text{PO}_4^-$  by ESI-MS studies in acetonitrile. Although ESI-MS studies are, by themselves, insufficient in determining the stoichiometry of a host-guest interactions, results of such experiments can serve as supporting evidence to the observed binding stoichiometry from solution phase experiments.<sup>64,65</sup> While experiments with  $\text{TBAH}_2\text{PO}_4$  only revealed evidence of a 1:1 complex (Supporting Information 3.2), similar experiments with  $\text{TBAH}_2\text{AsO}_4$  revealed a mass corresponding to  $[\text{M}+\text{NBu}_4+\text{H}_2\text{As}_2\text{O}_7]^-$ , which could provide additional evidence the formation of a 1:2 complex (Supporting Information 3.1, Figure 4). The preparative formation of pyroarsenate salts requires temperatures in an excess of 150  $^\circ\text{C}$ , typically for several hours, and they degrade rapidly in the presence of water.<sup>66</sup> Given that the ESI-source was held at 100  $^\circ\text{C}$ , it could be possible that the guest induces dehydration of  $\text{H}_2\text{AsO}_4^-$  at elevated temperatures or in the gas phase, due either to hydrogen bonding, or by simply holding two guest molecules in close proximity to one another. The formation of pyroarsenate induced by Receptor **3** in solution, however, could potentially explain the difference in binding energies between  $\text{H}_2\text{PO}_4^-$  and  $\text{H}_2\text{AsO}_4^-$ , as computational studies indicate that the formation of pyroarsenate is  $\sim 20$  kJ/mol less unfavorable than the formation of pyrophosphate.<sup>67</sup> Solution phase evidence to confirm or refute pyroarsenate formation, however, is currently elusive, and we are actively investigating the possibility of this phenomenon.

We also endeavored to further probe the binding interactions with all anions by  $^1\text{H}$ -NMR titration, as observation of similar binding interactions at different concentrations can serve as

further evidence for assigned binding behavior (Supporting Information 5).<sup>53</sup> As a result of aggregation and solubility issues observed in pure  $\text{MeCN-}d_3$  at concentrations greater than 0.25 mM, a mixed solvent system, 25%  $\text{CD}_2\text{Cl}_2$  in  $\text{MeCN-}d_3$ , was employed.



Adduct	m/z (Calc.)	m/z (Obs.)
$[\text{M}-\text{H}]^-$	1085.3295	1085.3326
$[\text{M}+\text{H}_2\text{AsO}_4]^-$	1227.2543	1227.2572
$[\text{M}+\text{NBu}_4+\text{H}_2\text{As}_2\text{O}_7]^-$	1592.4454	1592.4459

**Figure 4.** ESI-MS of Receptor **3** (95  $\mu\text{M}$ ) in the presence of 2

equiv. TBAH<sub>2</sub>AsO<sub>4</sub> in MeCN. The attached table shows observed masses and their assigned adducts.

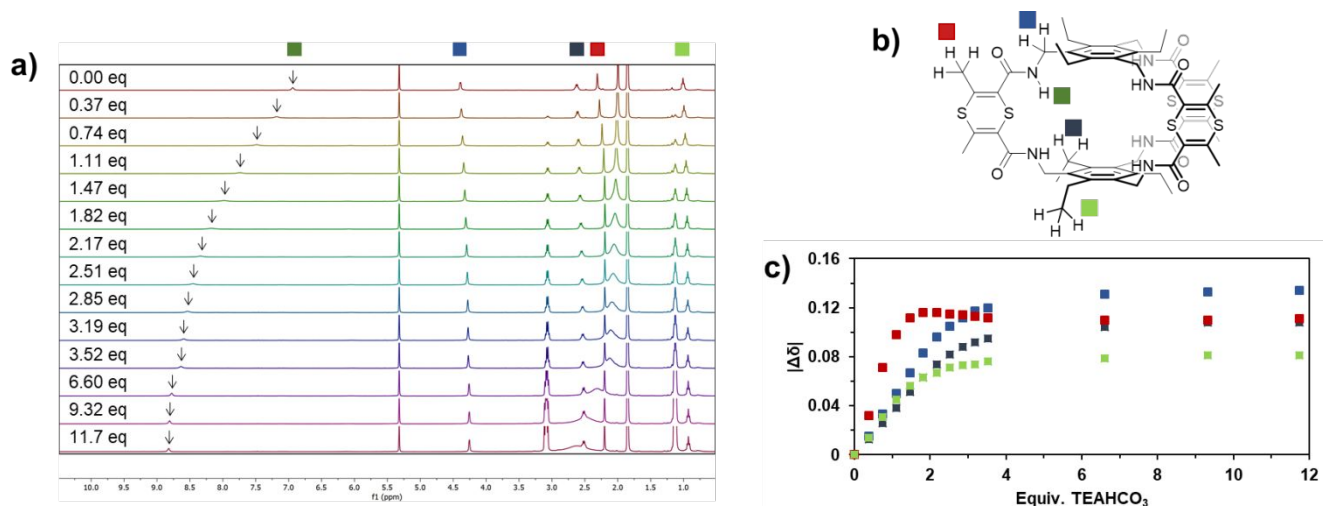


**Figure 5.** a) <sup>1</sup>H-NMR titration of Receptor **3** (1.02 mM) with TEAHCO<sub>3</sub> in 25% CDCl<sub>2</sub> in MeCN-*d*<sub>3</sub> (the arrow indicates the resonance associated with the amide proton), b) assignment of protons in Receptor **3**, c) derived changes in chemical shift for non-amide hydrogens.

A representative titration experiment with HCO<sub>3</sub><sup>-</sup> is shown in Figure 5. In all cases, the resonances corresponding to the amide protons shift downfield with increasing equivalents of anion, which is indicative of hydrogen bonding interactions. Interestingly, titration with TBAH<sub>2</sub>AsO<sub>4</sub> resulted in exceptionally broad receptor peaks, which may be a result of the inclusion of quadrupolar nuclei (Figure S110). This may implicate Receptor **3** as a probe for the presence of arsenate by <sup>1</sup>H-NMR. Due to the decreased solvent polarity, similar, but slightly higher, association constants were obtained for HSO<sub>4</sub><sup>-</sup> (Figure S112), and NO<sub>3</sub><sup>-</sup> (Figure S113). For experiments with HCO<sub>3</sub><sup>-</sup>, different values were obtained for *K*<sub>1:1</sub> and *K*<sub>1:2</sub> than from UV/Vis titration experiments, but data analysis indicated the same binding stoichiometry and similar value for β<sub>2</sub>.

In the case of Cl<sup>-</sup>, a small *K*<sub>1:2</sub> is observed (log*K*<sub>1:2</sub> ~ 1.0) that may arise due to ion pairing equilibria from both the higher concentration and less polar solvent system employed (Figure S114). <sup>1</sup>H-NMR titrations with OAc<sup>-</sup> provided a lower association constant, but such activity is unsurprising given that OAc<sup>-</sup> has a *K*<sub>1:1</sub> beyond the detection limit for <sup>1</sup>H-NMR experiments (Figure S108).<sup>53</sup> For H<sub>2</sub>PO<sub>4</sub><sup>-</sup>, <sup>1</sup>H-NMR titration revealed a *K*<sub>1:1</sub> that is greater than what was measured in our UV/Vis titration experiments (log*K*<sub>1:1</sub> ~ 4.6), as well as a relatively small *K*<sub>1:2</sub> (log*K*<sub>1:2</sub> ~ 3.4, logβ<sub>2</sub> ~ 8.1) (Figure S109). As evidenced by our experiments with arsenate and bicarbonate, the size of the binding site does not preclude the inclusion of two anionic species, and it may be that the slightly less polar solvent system induces further burying of the hydrophilic surface area of H<sub>2</sub>PO<sub>4</sub><sup>-</sup>, forming higher order complexes. Additionally, the switching of binding stoichiometry is not uncommon upon changing solvent polarity.<sup>64,68,69</sup> Finally, <sup>1</sup>H-NMR titrations with CN<sup>-</sup> were inconsistent with our UV/Vis experiments, but we also observed a change in solution color (colorless to orange), which may indicate some reaction of cyanide with the receptor, complicating the binding model (Figure S111). Such behavior was not observed at lower concentrations in the case of the UV/Vis experiment. See Supporting Information 5.1 for further discussion on the <sup>1</sup>H-NMR experiments.

The overall affinities of Receptor **3** with the anions surveyed are surprisingly high. Although Receptor **1** demonstrates high affinity for NO<sub>3</sub><sup>-</sup> and OAc<sup>-</sup> (log*K*<sub>1:1</sub> ~ 2.5 and 2.9 in 25% CD<sub>2</sub>Cl<sub>2</sub> in MeCN-*d*<sub>3</sub>), the overall anion affinity is significantly decreased compared to Receptor **3**.<sup>43</sup> We speculate that this may be due to repulsive interactions between the pyridine nitrogen and anionic guest. The sulfur atom, on the other hand, is bent out of the plane of the amide hydrogens, preventing such repulsive interactions, as observed from the crystal structure and DFT calculated geometry (Figure 2, Supporting Information 11, Figure S169). Additionally, modelling of Receptor **3** with either one or two molecules of H<sub>2</sub>AsO<sub>4</sub><sup>-</sup> or H<sub>2</sub>As<sub>2</sub>O<sub>7</sub><sup>2-</sup> indicated C-H hydrogen bonding interactions with the methyl groups on the 1,4-dithiin ring, which may enhance interactions with guests (Supporting Information 11, Figure S170-172). This increase in affinity is advantageous in that it could help to overcome the large solvation energy of anions, allowing binding in more polar solvents.

Additionally, it is important to note that Receptor **1** was not subjected to titration experiments with H<sub>2</sub>AsO<sub>4</sub><sup>-</sup> and its binding selectivity for H<sub>2</sub>PO<sub>4</sub><sup>-</sup> over H<sub>2</sub>AsO<sub>4</sub><sup>-</sup> is unknown. Most receptors that have been found to complex phosphate, in fact, have not been tested with arsenate. Due to the environmental and biological relevance of arsenate, we believe that this anion should become a more standard guest in the characterization of supramolecular receptors to help establish trends in arsenate-phosphate discrimination.

**Electrochemical Characterization.** 1,4-Dithiins, similar to thianthrenes, are known to undergo a reversible, single electron oxidation under anhydrous conditions.<sup>42</sup> As a result of the proximity of the redox-active moiety to the binding site as well as the planarization of 1,4-dithiin moieties upon single electron oxidation, we hypothesized that the inclusion of different anions could give rise to different electrochemical responses, such as varying cathodic perturbations in the observed *E*<sup>1/2</sup>.<sup>31</sup> In a solution of 0.1 M TBAPF<sub>6</sub> in MeCN, the macrocycle undergoes a single quasi-reversible oxidation event (Figure 6a, Supporting Information 7.1, Figure S124). Although Receptor **3** has limited solubility in pure acetonitrile, the addition of

TBAPF<sub>6</sub> allows for effective dissolution. In comparison with model compound **S5**, both are oxidized at similar potentials ( $E^{1/2} = 0.65$  V vs Fc/Fc<sup>+</sup>, **S5**,

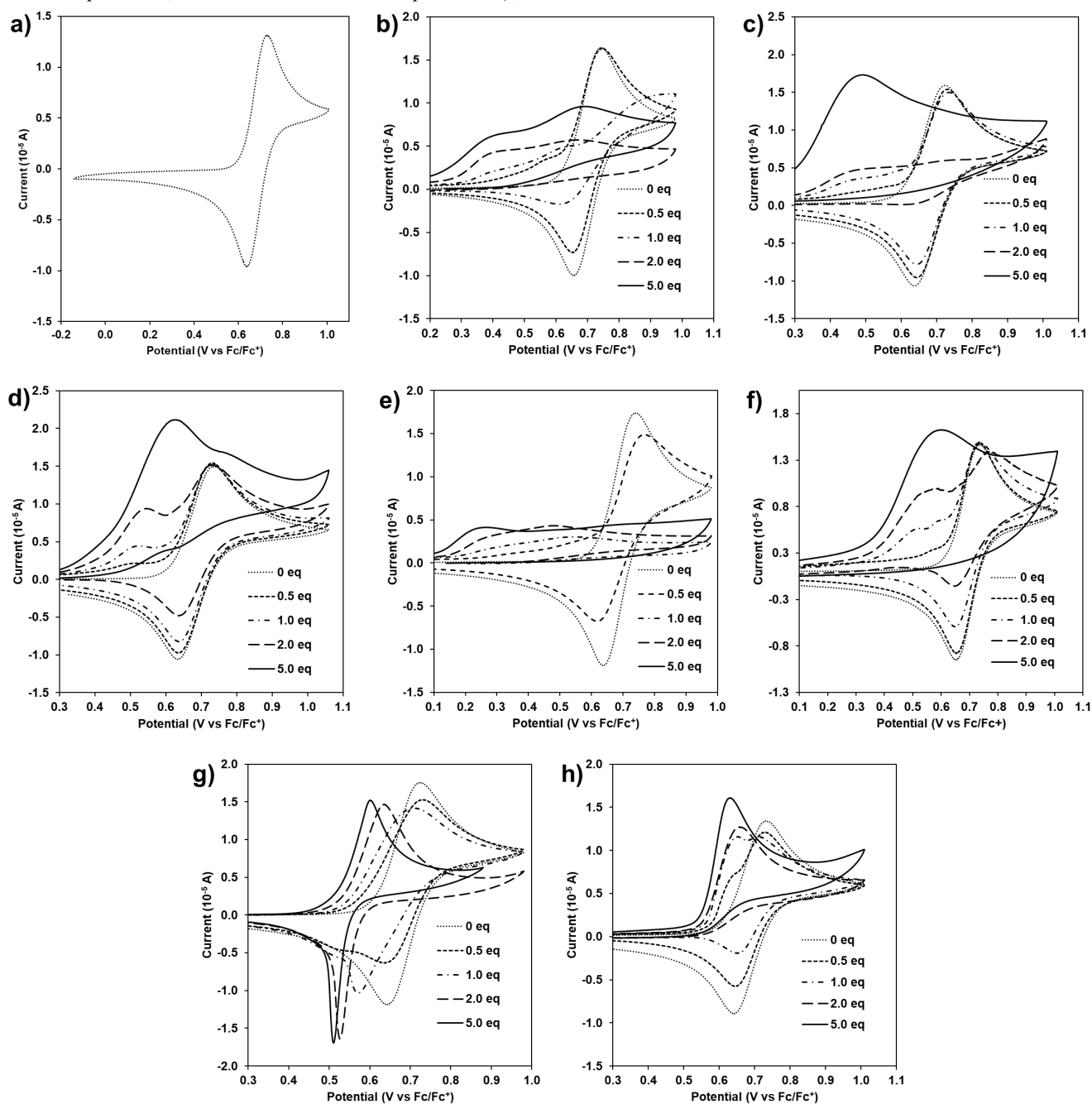


**Figure 6.** Cyclic voltammograms of Receptor **3** with a) no additive and varying equivalents of b) TBAH<sub>2</sub>AsO<sub>4</sub> c) TEAHCO<sub>3</sub> d) TBAOAc e) TBAH<sub>2</sub>PO<sub>4</sub> f) TBACN g) TBAHSO<sub>4</sub> and h) TBANO<sub>3</sub>. All measurements were performed in MeCN with 0.1 M TBAPF<sub>6</sub>, platinum working (0.031 cm<sup>2</sup>) and counter electrode and Ag wire pseudoreference electrode at 100 mV/s and were referenced to the Fc/Fc<sup>+</sup> redox couple.

$E^{1/2} = 0.71$  V vs Fc/Fc<sup>+</sup>, Figure S125), but the oxidation of Receptor **3** is kinetically slower, as indicated by the larger shift in peak potential with scan rate. To determine the electron transfer number for the oxidation of Receptor **3**, we performed chronoamperometry and cyclic voltammetry with a microelectrode. Analysis of the data as established by Amatore and coworkers indicated that the oxidation event involved a degenerate or near-degenerate transfer of three electrons (Supporting Information 7.2).<sup>70</sup> Formation of a tricationic complex would foster stronger interactions with guests via

electrostatic attraction, further enhancing the affinity of the oxidized complex with each anion.

Next, the electrochemical behavior of Receptor **3** in the presence of various anions was surveyed (Figure 6b-h). Due to the relatively low oxidation potential of chloride ( $E^{1/2} = 0.52$  V vs Fc/Fc<sup>+</sup>, Figure S132), it was excluded from this study. Receptor **3** exhibits complex oxidation behavior for each anionic guest, which we believe results from unique binding behavior of the oxidized receptor, changes in the  $E^{1/2}$  and electron transfer kinetics upon complexation, and subsequent

reaction of the anion with Receptor **3** upon oxidation. Upon addition of  $\text{NO}_3^-$ , the oxidation wave shifts to less positive potentials and becomes chemically irreversible (Figure 6h). This can be rationalized by the oxidation of the tri-radical cation by nitrate, a known behavior in thianthrene radical cations.<sup>71</sup> The addition of  $\text{H}_2\text{PO}_4^-$ ,  $\text{H}_2\text{AsO}_4^-$ ,  $\text{HCO}_3^-$ ,  $\text{CN}^-$ , and  $\text{OAc}^-$  gave irreversible redox couples as well, but analysis of subsequent scans demonstrated varying degrees of precipitation on the electrode surface (Figure 6b-f, Supporting Information 7.4). In the case of  $\text{H}_2\text{PO}_4^-$  (Figure S135),  $\text{HCO}_3^-$  (Figure S145) and  $\text{CN}^-$  (Figure S139) acquisition of subsequent scans by cyclic voltammetry resulted in little signal, indicating the formation of an insulating film on the electrode surface. Subsequent scans, however, in the case of  $\text{NO}_3^-$  (Figure S141),  $\text{H}_2\text{AsO}_4^-$  (Figure S137), and  $\text{OAc}^-$  (Figure S143), gave similar voltammograms but with lower current, indicating that the fidelity of the electrode surface is maintained, but that Receptor **3** proximate to the electrode surface was consumed due to an irreversible chemical reaction with the anionic guest. Finally, while  $\text{HSO}_4^-$  exhibited a moderate association constant with the neutral receptor as determined by UV/Vis titrations, we found that addition of bisulfate caused dramatic changes in the shape of both the oxidation and reduction waves while maintaining chemical reversibility (Figure 6g, Figure S133). Interestingly, in the case of  $\text{NO}_3^-$ , two-wave behavior is observed, (Figure 6h). Such behavior is indicative of slow-exchange interactions and is potentially useful in the differentiation of anions in a similar fashion that has been described for slow host-guest exchange in NMR studies.<sup>17</sup> In other cases, such as  $\text{H}_2\text{AsO}_4^-$ ,  $\text{H}_2\text{PO}_4^-$ ,  $\text{OAc}^-$ ,  $\text{HCO}_3^-$ , and  $\text{CN}^-$  as many as three distinct oxidation waves can be observed after addition of various equivalents of the anion (Figure 6b-f). Due to the irreversible nature of these redox couples, exact analysis of oxidation event is difficult, and we abandoned further electrochemical experiments due to the high reactivity of Receptor **3** in its oxidized form. Additionally, more complex mechanisms, such as ECE or the loss of degeneracy in the oxidation of Receptor **3**, may be at play, further complicating the response.

The results of the electrochemical anion titrations are summarized in Table 2. Although the magnitude of the change in peak potential is similar to the more common strategy of appending receptors with well-known redox transducers, such as ferrocene, changes in peak shape and degree of chemical reversibility vary widely based on the identity of the anionic guest. In our case, we also believe the conformational activity of the electroactive moiety may participate in enhancing the response towards anions. Geometry of the triply oxidized host, as generated from DFT calculations, indicate that the planarization of the 1,4-dithiin moieties generates a cationic binding site of unique size as compared to the neutral receptor, which may aid in enhancing the change in association constant of the oxidized receptor (Supporting Information 11, Figure S173). Interestingly, we found that Receptor **3** exhibits a moderate association constant to the supporting electrolyte,  $\text{TBAPF}_6$  ( $\log K_{1:1} \sim 3.7$ , Supporting Information 7.3, Figure S130-131). In spite of this, the addition of other anionic guests, even those with comparable  $K_a$ , gave altered voltammograms. This may indicate that binding occurs almost solely with the oxidized host under the conditions for electrochemical measurements. Finally, we found that after an addition of five equivalents of  $\text{TBAHSO}_4$ , with a shift in  $E^{1/2}$  of 126 mV and a three electron process, that a binding enhancement factor (BEF)

of  $2.5 \times 10^6$  could be estimated.<sup>31</sup> Moreover, larger perturbation in the peak potential of oxidation was observed with other anions, but lack of a return wave precluded an estimation of the BEF. Although the use of 1,4-dithiins as redox transducers may be too sensitive for practical applications in the presence of nucleophilic species, the incorporation of multiple redox-active moieties adjacent to the binding site could give molecules with sufficiently high ion affinities when oxidized to effectively bind to anions in polar media.

## Conclusion

In conclusion, we have synthesized and characterized an anion receptor with novel 1,4-dithiin moieties. The receptor shows high selectivity and affinity towards  $\text{HCO}_3^-$  and  $\text{H}_2\text{AsO}_4^-$ , which were observed to bind in a 1:2 host:guest binding mode. Additionally,  $\text{H}_2\text{AsO}_4^-$  was found to undergo different binding behavior with Receptor **3** than  $\text{H}_2\text{PO}_4^-$ , an uncommon characteristic given the two anions similar size and properties. Further analysis by cyclic voltammetry revealed unique responses upon the addition of anionic guests, but due to the high reactivity of Receptor **3** when oxidized, deconvolution of the response proved difficult in many cases. Due to the interest in the detection and binding of arsenate and the lack of effective strategies towards selective complexation, we hope this report will encourage other researchers to include this anion in their studies to help establish trends in arsenate-phosphate discrimination. Future experiments in our laboratory will involve the further synthesis and characterization of anion receptors with potential application in the monitoring of environmentally relevant anion contaminants.

**Table 2. Summary of electrochemical response upon towards various anions.**

Anion <sup>a</sup>	$\Delta E_{\text{ox}}$ (mV) <sup>b</sup>
$\text{H}_2\text{AsO}_4^-$	-334 <sup>c</sup>
$\text{HCO}_3^-$ <sup>d</sup>	-235
$\text{OAc}^-$	-105
$\text{H}_2\text{PO}_4^-$	-480
$\text{CN}^-$	-142
$\text{HSO}_4^-$	-118
$\text{NO}_3^-$	-102
$\text{Cl}^-$	N/D <sup>e</sup>

<sup>a</sup> Tetrabutylammonium salts were employed. <sup>b</sup> Change in peak potential of the oxidation event upon addition of 5 eq of anion. <sup>c</sup> Two oxidation events are observed. The more cathodic peak is reported here. <sup>d</sup> Tetraethylammonium bicarbonate was employed. <sup>e</sup> Not determined

## EXPERIMENTAL SECTION

**General Experimental Considerations.** All reagents were purchased from commercial sources and used without further purification unless otherwise specified. Anhydrous tetrahydrofuran (THF) and dichloromethane ( $\text{CH}_2\text{Cl}_2$ ) were purified using an Inert solvent purification system by passage through two alumina columns and were stored in a Schlenk flask over 4 Å molecular sieves under an argon atmosphere. Tetrabutylammonium hexafluorophosphate for electrochemical analysis was recrystallized from EtOH three times and dried in a vacuum oven at 60 °C. All chemical manipulations were



performed under an argon atmosphere in flame-dried glassware unless otherwise specified. Reported reaction temperatures refer to the temperature of external water or oil baths.

Chromatographic purifications were performed with a Biotage Isolera using Biotage SNAP Ultra columns with the specified solvent gradient. Typically, columns were performed with one column volume of the initial solvent gradient, followed by a linear gradient over ten column volumes to the final solvent composition, followed by an additional two column volumes at the final solvent composition.

NMR spectra were recorded on either a 400 MHz Bruker Avance-III HD Nanobay spectrometer, 500 MHz Bruker Avance Neo spectrometer, or 600 MHz Bruker Avance Neo spectrometer. Chemical shifts  $\delta$  are reported in ppm downfield from tetramethylsilane by referencing to residual solvent signals (CDCl<sub>3</sub>:  $\delta$  <sup>1</sup>H 7.26 ppm,  $\delta$  <sup>13</sup>C 77.16 ppm; DMSO-*d*<sub>6</sub>:  $\delta$  <sup>1</sup>H 2.50 ppm,  $\delta$  <sup>13</sup>C 39.52 ppm; CD<sub>3</sub>CN:  $\delta$  <sup>1</sup>H 1.94,  $\delta$  <sup>13</sup>C 118.26). Coupling constants *J* are listed in Hz with multiplicities *s* (singlet), *d* (doublet), *t* (triplet), *q* (quartet), and *m* (multiplet). Mass spectra were obtained on a JEOL AccuTOF system equipped with either a DART (DART-MS) or ESI (ESI-MS) source or an Agilent 6545 Q-TOF equipped with an AJS-ESI (Q-TOF-ESI-MS) source.

**Titration Experiments.** All UV/Vis titrations were carried out on an Agilent Cary-4000 UV/Vis spectrometer, recording from 500-200 nm at intervals of 0.5 nm. Tetrabutylammonium salts were stored in a vacuum desiccator prior to titration. UV/Vis titrations were carried out in HPLC grade MeCN in 1 cm cuvettes at the specified host concentration. Host concentration was determined using Beer's law absorbance of 292 nm, which is linearly correlated with concentration (Figure S23). Anionic guests were dissolved in a solution of the host to keep host concentration constant over the course of the experiment. Guests were added using either 10 or 50  $\mu$ L syringes (Hamilton), followed by manual agitation for 5-10 s. Association constants were then determined using SIVVU with absorbance data from 275-500 nm.

<sup>1</sup>H-NMR titrations were performed in 25% CD<sub>2</sub>Cl<sub>2</sub> in CD<sub>3</sub>CN. Anionic guests were dissolved in a solution of the host to keep host concentration constant over the course of the titration. Solutions of the anion were added in 5 or 25  $\mu$ L aliquots using either 10 or 50  $\mu$ L syringes (Hamilton) followed by manual agitation for 10-15 seconds followed by immediate measurement by <sup>1</sup>H-NMR at the specified field. In all cases, the spectra were referenced to residual CDHCl<sub>2</sub> ( $\delta$  = 5.32 ppm).

**Electrochemical Experiments.** Electrochemical experiments were performed in a nitrogen filled glovebox (O<sub>2</sub> < 20 ppm, H<sub>2</sub>O < 2 ppm) with a BioLogic SP-150 potentiostat. Platinum working electrodes (2 mm diameter and 10  $\mu$ M) were polished using first suspensions of 1.0  $\mu$ m, then 0.3  $\mu$ m, then 0.05  $\mu$ m alumina in water on a polishing pad followed by sonication in methanol to remove excess alumina and then chemical polishing by cycling the electrode in 1 M H<sub>2</sub>SO<sub>4</sub> over the potential window of water until the resulting traces overlapped. The electrode was then rinsed with methanol and blown dry with nitrogen before being transferred into the glovebox. A platinum wire was used as the counter electrode. A silver pseudoreference electrode was used, and all measurements were referenced to Fc/Fc<sup>+</sup>. All titration experiments were performed at 1.0 mM of active material in MeCN with 0.1 M TBAPF<sub>6</sub> as a supporting electrolyte. In the case that the oxidation was chemically irreversible, which is the case with all anions except for TBAHSO<sub>4</sub>, the first scan is

reported. In the case of TBAHSO<sub>4</sub>, the third scan is reported, which is similar to the first two scans.

**ESI-MS Experiments.** Electrospray ionization (ESI) binding experiments were carried out on a JEOL Accu-TOF equipped with an ESI source. All ions were observed in negative mode with the orifice and desolvating chambers held at 100 °C. Samples were run via direct infusion at the specified concentration at a rate of 1.0 mL/h using a syringe pump. All experiments were run holding the host concentration at approximately 100  $\mu$ M in acetonitrile.

**Computational Studies.** Theoretical calculations were carried out with the Spartan '18 (1.4.4, Wave function Inc, Irvine CA) software packages on a computer operating with Windows 10 OS. Geometry optimizations were performed with density functional theory (DFT) calculations using the B3LYP functional with the 6-31G\* basis set in the gas phase. Frequency calculations were performed to confirm structures were at a local energy minimum. Outputs were visualized with CYLview.<sup>72</sup>

### Synthetic Procedures

*Diethyl 2,2'-thiobis(3-oxobutanoate) (5)* **Caution:** *This reaction produces stoichiometric amounts of HCl gas and must be performed in a fume hood or similarly well-vented area.* The title compound was prepared according to a modified literature procedure.<sup>45</sup> To a round bottom flask open to the atmosphere, ethyl acetoacetate (4) (10.0 mL, 78.5 mmol, 1.0 equiv.) and hexanes (16 mL) were added. The mixture was then heated to 40 °C, upon which the solution became homogenous. Disulfur dichloride (3.14 mL 39.2 mmol, 0.5 equiv.) was then added in one portion. After 1-2 min, the solution developed a yellow color and began to bubble vigorously. After the bubbling had subsided, the solution was allowed to react for a further 30 min, over which a solid precipitated. The reaction was then cooled in an ice bath, and the white solid was collected by vacuum filtration, washed first with hexanes and then water, and subsequently dried under vacuum at 50 °C to remove residual water. The solid was purified by recrystallization in acetone (25 mL) to give the target compound as colorless needles (4.59 g, 15.8 mmol, 40%). <sup>1</sup>H NMR (500 MHz, CDCl<sub>3</sub>)  $\delta$  13.40 (s, 2H), 4.23 (q, *J* = 7.1 Hz, 4H), 2.42 (s, 6H), 1.30 (t, *J* = 7.1 Hz, 6H). <sup>13</sup>C{<sup>1</sup>H} NMR (126 MHz, CDCl<sub>3</sub>)  $\delta$  181.4, 172.9, 95.1, 61.4, 21.1, 14.3. HRMS (DART-MS) *m/z*: [M+H]<sup>+</sup> Calcd for C<sub>12</sub>H<sub>19</sub>O<sub>6</sub>S<sup>+</sup> 291.0897; Found 291.0900.

*Diethyl 3,5-dimethyl-1,4-dithiine-2,6-dicarboxylate (7)* THF (50 mL) was added to round bottom flask containing sodium hydride (3.31 g, 60% dispersion in mineral oil, 82.8 mmol, 3.0 equiv.). The mixture was cooled to 0 °C, and compound 5 (8.0 g, 27.6 mmol, 1.0 equiv.) was added as a solution in THF (125 mL) via cannula transfer over approximately 10 min, resulting in the evolution of H<sub>2</sub> gas. After completion of the addition, the mixture was allowed to stir for a further 30 min at 0 °C, after which tosyl anhydride (19.8 g, 60.7 mmol, 2.2 equiv.) was added as a solution in THF (150 mL) via cannula transfer over approximately 10 min, during which the reaction mixture became viscous. The reaction was then allowed to warm to room temperature. After conversion was complete, as judged by TLC (approximately 3 h), the reaction was quenched slowly with the addition of water (20 mL) and then 4 M HCl (20 mL). The reaction was concentrated under reduced pressure to a total volume of about 100 mL. The resulting mixture was then extracted with diethyl ether (3 x 100 mL), and then the organic layers were combined, washed with saturated NaHCO<sub>3</sub> (100 mL) and brine (100 mL), dried over Na<sub>2</sub>SO<sub>4</sub>, filtered, and

concentrated under reduced pressure to give approximately 15 g of a red oil containing compound **6** as mixture of isomers. The mixture was used without purification in the next step. The red oil was dissolved in EtOH (125 mL), and sodium sulfide nonahydrate (4.96 g, 20.7 mmol, 0.75 equiv.) was added in one portion, resulting in the appearance of an orange solution and the precipitation of a solid. After 1.5 h, CH<sub>2</sub>Cl<sub>2</sub> (125 mL) was added to further precipitate additional salts, and the mixture was filtered through a bed of celite, and the volatiles were removed under reduced pressure. The dark oil was then purified by flash chromatography (1% → 15% EtOAc in hexanes) to give the title compound as an orange oil that solidifies upon storage at 2-5 °C (5.08 g, 17.6 mmol, 64%). <sup>1</sup>H NMR (400 MHz, CDCl<sub>3</sub>) δ 4.25 (q, *J* = 7.1 Hz, 4H), 2.41 (s, 6H), 1.32 (t, *J* = 7.2 Hz, 6H). <sup>13</sup>C{<sup>1</sup>H} NMR (101 MHz, CDCl<sub>3</sub>) δ 162.9, 149.6, 122.3, 61.9, 22.7, 14.3. HRMS (DART-MS) *m/z*: [M+H]<sup>+</sup> Calcd for C<sub>12</sub>H<sub>17</sub>O<sub>4</sub>S<sub>2</sub><sup>+</sup> 289.0563; Found 289.0558.

**3,5-Dimethyl-1,4-dithiine-2,6-dicarboxylic acid (8)** Potassium hydroxide (85%, 2.90 g, 44.0 mmol, 2.5 equiv.) pellets were crushed using a mortar and pestle and then dissolved in EtOH (35 mL). The ethanolic KOH was then added to compound **7** (5.08 g, 17.6 mmol, 1.0 equiv.) in one portion, and the mixture was then heated to 50 °C with strong stirring. Within 10 min a solid had precipitated. The reaction was allowed to proceed for a further 1.5 h, after which the mixture was cooled to 0 °C. The solid was collected by filtration, washed several times with EtOH, and then dissolved in water (50 mL). The product was precipitated with the addition of 4 M HCl until the solution had a pH < 1. The product was collected by filtration, washed with water, and dried at 60 °C under vacuum to give the title compound as a light orange powder (2.43 g, 10.5 mmol, 60%). <sup>1</sup>H NMR (500 MHz, DMSO-*d*<sub>6</sub>) δ 13.43 (s, 2H), 2.34 (s, 6H). <sup>13</sup>C{<sup>1</sup>H} NMR (126 MHz, DMSO-*d*<sub>6</sub>) δ 163.7, 146.9, 123.0, 22.1. HRMS (Q-TOF-ESI-MS) *m/z*: [M-H]<sup>-</sup> Calcd for C<sub>8</sub>H<sub>7</sub>O<sub>4</sub>S<sub>2</sub><sup>-</sup> 230.9791; Found 230.9793.

**3,5-Dimethyl-1,4-dithiine-2,6-dicarbonyl dichloride (9)**

**General Procedure:** A round bottom flask was charged with compound **8** (1.0 equiv.) and CH<sub>2</sub>Cl<sub>2</sub> (0.2 M), giving a suspension. DMF (1-2 drops) and oxalyl chloride (2.5 equiv.) were then added, resulting in the evolution of gas. After 2 h, the solution became homogenous, and the volatiles were removed under reduced pressure, giving an orange solid. For all transformations, the conversion of diacid to acyl chloride was assumed to be quantitative. The diacyl chloride **9** was prepared from diacid **8** directly when needed. <sup>1</sup>H NMR (500 MHz, CDCl<sub>3</sub>) δ 2.46 (s, 6H). <sup>13</sup>C{<sup>1</sup>H} NMR (126 MHz, CDCl<sub>3</sub>) δ 163.0, 156.9, 125.3, 23.3.

**1,3,5-Tris(bromomethyl)-2,4,6-triethylbenzene (S2)** The title compound was prepared in accordance to a literature procedure.<sup>73</sup> 1,3,5-Triethylbenzene (**S1**) (10.0 mL, 53.1 mmol, 1.00 equiv.) and paraformaldehyde (16.8 g, 560 mmol, 10 equiv.) were dissolved in a solution of 30% HBr in HOAc (100 mL). Zinc bromide (19.8 g, 87.8 mmol, 1.65 equiv.) was added, and the reaction was then brought to 90 °C and stirred overnight. The mixture was cooled to room temperature, and the solid was collected by vacuum filtration and washed with water to give the title compound as an off white powder (21.1 g, 47.8, 90%). <sup>1</sup>H- and <sup>13</sup>C-NMR spectra were consistent with those reported in the literature.<sup>73</sup> <sup>1</sup>H NMR (500 MHz, CDCl<sub>3</sub>) δ 4.58 (s, 6H), 2.95 (q, *J* = 7.6 Hz, 6H), 1.34 (t, *J* = 7.6 Hz, 9H). <sup>13</sup>C{<sup>1</sup>H} NMR (126 MHz, CDCl<sub>3</sub>) δ 145.2, 132.8, 28.7, 22.9, 15.8.

**1,3,5-Tris(azidomethyl)-2,4,6-triethylbenzene (S3) Caution:** Azides are potentially explosive. While we never experienced any explosions with the title compound, appropriate hazards should be observed when preparing and working with it. The title compound was prepared according to a modified literature procedure.<sup>74</sup> Compound **S2** (21.1 g, 47.8 mmol, 1.0 equiv.) was dissolved in DMF (100 mL). Sodium azide (10.3 g, 158 mmol, 3.3 equiv.) was then added in one portion, and the solution became homogenous over the course of 10 min. After 2 d, water (50 mL) was added, and the mixture was extracted with Et<sub>2</sub>O (3 x 100 mL). The organic layers were combined and washed with water (4 x 50 mL) and brine (100 mL), dried with MgSO<sub>4</sub>, filtered and concentrated under reduced pressure to give the title compound as a white powder (14.8 g, 45.2 mmol, 95%). <sup>1</sup>H- and <sup>13</sup>C-NMR spectra were consistent with those reported in the literature.<sup>74</sup> <sup>1</sup>H NMR (400 MHz, CDCl<sub>3</sub>) δ 4.49 (s, 6H), 2.85 (q, *J* = 7.6 Hz, 6H), 1.24 (t, *J* = 7.6 Hz, 9H). <sup>13</sup>C{<sup>1</sup>H} NMR (101 MHz, CDCl<sub>3</sub>) δ 145.1, 130.1, 48.1, 23.3, 15.9.

**(2,4,6-Triethylbenzene-1,3,5-triyl)trimethanamine (10)** The title compound was prepared according to a modified literature procedure.<sup>75</sup> A round bottom flask was charged with 5% palladium on carbon (1.07 g) and MeOH (100 mL). The reaction vessel was then evacuated and refilled with hydrogen 5 times. A suspension of compound **S3** (14.8 g, 45.2 mmol, 1.0 equiv.) in MeOH (100 mL) was added, and the vessel was subsequently evacuated and refilled with hydrogen 5 times. The reaction was purged with hydrogen several times until conversion was complete as observed by <sup>1</sup>H-NMR (typically 3 d). After the reaction was complete, the reaction mixture was filtered through a pad of celite. The filtrate was then concentrated under reduced pressure, giving the title compound as a pink solid (10.5 g, 42.1 mmol, >95%). <sup>1</sup>H and <sup>13</sup>C-NMR spectra were consistent with those reported in the literature.<sup>75</sup> <sup>1</sup>H NMR (500 MHz, CDCl<sub>3</sub>) δ 3.87 (s, 6H), 2.82 (q, *J* = 7.5 Hz, 6H), 1.37 (s, 6H), 1.23 (t, *J* = 7.5 Hz, 9H). <sup>13</sup>C{<sup>1</sup>H} NMR (126 MHz, CDCl<sub>3</sub>) δ 140.5, 137.6, 39.8, 22.7, 16.9.

**Di-tert-butyl ((5-(((benzyloxy)carbonyl)amino)methyl)-2,4,6-triethyl-1,3-phenylene)bis(methylene)dicarbamate (S4)** The title compound was prepared according to a modified literature procedure.<sup>46</sup> Compound **10** (4.00 g, 16.0 mmol, 1.0 equiv.) and sodium hydroxide (960 mg, 24.0 mmol, 1.5 equiv.) were added to a round bottom flask and dissolved in dioxane (80 mL) and water (80 mL), and the solution was cooled to 0 °C. Benzylchloroformate (3.87 mL, 27.2 mmol, 1.7 equiv.) and di-tert-butyl dicarbonate (11.0 g, 50.5 mmol, 3.15 equiv.) were dissolved in a minimal amount of dioxane to give a total volume of 20 mL and added over 4 h via syringe pump. After the addition was complete, the reaction was allowed to come to room temperature and stirred for a further 2 h. The dioxane was then removed under reduced pressure, and the resulting aqueous layer was extracted with CH<sub>2</sub>Cl<sub>2</sub> (3 x 50 mL). The organic layers were combined, washed with brine (100 mL), filtered, and concentrated under reduced pressure to give an orange oil, which is then purified by flash chromatography (5% → 30% EtOAc in hexanes with 1% v/v Et<sub>3</sub>N) to give the title compound as a white solid (2.42 g, 4.14 mmol, 26%). <sup>1</sup>H- and <sup>13</sup>C-NMR spectra were consistent with those reported in the literature.<sup>46</sup> <sup>1</sup>H NMR (500 MHz, DMSO-*d*<sub>6</sub>) δ 7.40 – 7.24 (m, 5H), 7.16 (t, *J* = 4.8 Hz, 1H), 6.53 (t, *J* = 4.8 Hz, 2H), 5.04 (s, 2H), 4.25 (d, *J* = 4.9 Hz, 2H), 4.18 (d, *J* = 4.9 Hz, 2H), 2.72 – 2.61 (m, 6H), 1.38 (s, 18H), 1.05 (t, *J* = 7.4 Hz, 9H). <sup>13</sup>C{<sup>1</sup>H} NMR (126 MHz, DMSO-*d*<sub>6</sub>) δ 155.8, 155.2, 143.0, 142.7, 137.2, 132.2,

131.80, 128.3, 127.7, 127.6, 77.7, 65.3, 38.7, 38.1, 28.3, 22.5, 22.4, 16.2, 16.1.

*Di-tert-butyl ((5-(aminomethyl)-2,4,6-triethyl-1,3-phenylene)bis(methylene)) dicarbamate (11)* The title compound was prepared according to a modified literature procedure.<sup>46</sup> A round bottom flask was charged with 5% palladium on carbon (172 mg) and MeOH (40 mL). The reaction vessel was then evacuated and refilled with hydrogen 5 times. A solution of compound **S4** (2.27 g, 3.89 mmol, 1.0 equiv.) in MeOH (40 mL) was added, and the vessel was then evacuated and refilled with hydrogen 5 times. The reaction was repeatedly purged with hydrogen until conversion was complete as observed by <sup>1</sup>H-NMR (around 2.5 h). After the reaction was complete, the reaction was filtered through a pad of celite. The filtrate was then concentrated under reduced pressure, giving the title compound as a white solid (1.75 g, 3.89 mmol, quant.). <sup>1</sup>H and <sup>13</sup>C-NMR spectra were consistent with those reported in the literature.<sup>46</sup> <sup>1</sup>H NMR (500 MHz, DMSO-*d*<sub>6</sub>) δ 6.61 (t, *J* = 4.8 Hz, 2H), 4.17 (d, *J* = 4.8 Hz, 4H), 3.70 (s, 2H), 2.71 (q, *J* = 7.5 Hz, 4H), 2.64 (q, *J* = 7.5 Hz, 2H), 1.38 (s, 18H), 1.10 (t, *J* = 7.5 Hz, 6H), 1.06 (t, *J* = 7.3 Hz, 3H). <sup>13</sup>C{<sup>1</sup>H} NMR (126 MHz, DMSO-*d*<sub>6</sub>) δ 155.2, 141.9, 141.8, 136.9, 132.0, 77.6, 38.2, 28.3, 22.4, 22.1, 16.5, 16.3.

*Tetra-tert-butyl (((((3,5-dimethyl-1,4-dithiine-2,6-dicarbonyl)bis(azanediyl))bis(methylene))bis(2,4,6-triethylbenzene-5,1,3-triyl))tetrakis(methylene)tetracarbamate (12)* A round bottom flask containing compound **11** (1.75 g, 3.89 mmol, 2.1 equiv.) and triethylamine (0.65 mL, 4.6 mmol, 2.5 equiv.) in CH<sub>2</sub>Cl<sub>2</sub> (10 mL) was cooled to 0 °C. In a separate flask, diacyl chloride **9** that was freshly prepared from diacid **8** (430 mg, 1.85 mmol, 1.0 equiv.) was dissolved in CH<sub>2</sub>Cl<sub>2</sub> (10 mL) and added dropwise to the solution of compound **11**. After the addition was complete, the reaction was allowed to come to room temperature and stir overnight. The solution was then poured into 1 M HCl (40 mL), and the layers were separated. The aqueous layer was further extracted with CH<sub>2</sub>Cl<sub>2</sub> (2 x 40 mL), and the organic layers were combined, washed with brine, dried over Na<sub>2</sub>SO<sub>4</sub>, filtered, and concentrated under reduced pressure to give an orange residue, which was purified by flash chromatography (0 → 3% MeOH in CH<sub>2</sub>Cl<sub>2</sub>) to give the title compound as an orange solid (1.62 g, 1.48 mmol, 80%). <sup>1</sup>H NMR (500 MHz, MeCN-*d*<sub>3</sub>) δ 6.62 (t, *J* = 4.8 Hz, 2H), 5.18 (s, 4H), 4.43 (d, *J* = 4.8 Hz, 4H), 4.29 (d, *J* = 5.0 Hz, 8H), 2.74 (q, *J* = 7.5 Hz, 4H), 2.69 (q, *J* = 7.5 Hz, 8H), 2.26 (s, 6H), 1.41 (s, 36H), 1.15 (t, *J* = 7.4 Hz, 6H), 1.10 (t, *J* = 7.4 Hz, 12H). <sup>13</sup>C{<sup>1</sup>H} NMR (126 MHz, MeCN-*d*<sub>3</sub>) δ 164.0, 156.5, 144.8, 144.5, 133.7, 132.3, 125.1, 79.4, 39.4, 39.0, 28.6, 23.6, 21.9, 16.6. HRMS (Q-TOF-ESI-MS) *m/z*: [M+H]<sup>+</sup> Calcd for C<sub>58</sub>H<sub>91</sub>N<sub>6</sub>O<sub>10</sub>S<sub>2</sub><sup>+</sup> 1095.6233; Found 1095.6210.

*N<sup>2</sup>,N<sup>6</sup>-Bis(3,5-bis(aminomethyl)-2,4,6-triethylbenzyl)-3,5-dimethyl-1,4-dithiine-2,6-dicarboxamide·4 HCl (13)* Compound **12** (1.553 g, 1.42 mmol, 1.0 equiv.) was dissolved in 4 M HCl in dioxane (12 mL), resulting in the formation of an orange precipitate. The reaction was allowed to stir for 2 h, after which isopropanol was added to dissolve all materials, and the volatiles were removed under reduced pressure, giving the title compound as a light orange powder (1.18 g, 1.40 mmol, 98%). <sup>1</sup>H NMR (600 MHz, DMSO-*d*<sub>6</sub>) δ 8.40 (s, 12H), 8.30 (t, *J* = 4.9 Hz, 2H), 4.39 (d, *J* = 4.5 Hz, 4H), 4.03 (s, 8H), 2.78 (q, *J* = 6.9 Hz, 12H), 2.14 (s, 6H), 1.11 (t, *J* = 7.3 Hz, 18H). <sup>13</sup>C{<sup>1</sup>H} NMR (151 MHz, DMSO-*d*<sub>6</sub>) δ 163.3, 145.3, 144.4, 139.3, 132.3, 128.8, 125.0, 37.5, 36.0, 23.2, 22.8, 21.6, 15.9, 15.9. HRMS (Q-

TOF-ESI-MS) *m/z*: [M+H]<sup>+</sup>  
Calcd for C<sub>38</sub>H<sub>59</sub>N<sub>6</sub>O<sub>2</sub>S<sub>2</sub><sup>+</sup> 695.4135; Found 695.4135.

**Receptor 3** In a 1 L round bottom flask, compound **13** (400 mg, 0.476 mmol, 1.0 equiv.) was dissolved in CHCl<sub>3</sub> (300 mL) and triethylamine (0.67 mL, 4.8 mmol, 10 equiv.), and the mixture was brought to 45 °C. Diacyl chloride **9** was prepared according to the general procedure using diacid **8** (221 mg, 0.951 mmol, 2.0 equiv.) and was then dissolved in CHCl<sub>3</sub> (25 mL) and taken up into a glass syringe. Diacyl chloride **9** was added to the reaction mixture over 8 h via syringe pump. After the addition was complete, the reaction was stirred for a further 20 h, and was then allowed to cool to room temperature. The volume of the reaction was reduced to approximately 50 mL under reduced pressure, and the solution was washed with 1 M HCl (50 mL). The aqueous layer was then extracted with CH<sub>2</sub>Cl<sub>2</sub> (2 x 50 mL), and the organic layers were combined and washed with 10% NaOH (100 mL), dried over Na<sub>2</sub>SO<sub>4</sub>, filtered, and concentrated under reduced pressure to give an orange solid. The residue was then purified by flash chromatography (15% → 25% Acetone in PhMe, then 0 → 100% EtOAc in hexanes) to give the title compound as a solvate. To remove residual solvent, the compound was sonicated in PhMe (5 mL) and the PhMe removed under pressure. This procedure is repeated 5 times to give the title compound as a pale yellow solid (104 mg, 0.0956 mmol, 20%). <sup>1</sup>H NMR (600 MHz, CDCl<sub>3</sub>) δ 6.22 (t, *J* = 4.8 Hz, 6H), 4.53 (d, *J* = 4.9 Hz, 12H), 2.66 (q, *J* = 7.5 Hz, 12H), 2.59 (s, 18H), 1.21 (t, *J* = 7.5 Hz, 18H). <sup>13</sup>C{<sup>1</sup>H} NMR (151 MHz, CDCl<sub>3</sub>) δ 162.6, 149.6, 145.6, 131.7, 119.7, 39.0, 23.6, 23.4, 15.9. HRMS (ESI-MS) *m/z*: [M+H]<sup>+</sup> Calcd for C<sub>54</sub>H<sub>65</sub>N<sub>6</sub>O<sub>6</sub>S<sub>6</sub><sup>+</sup> 1085.3295; Found 1085.3342.

*N<sup>2</sup>,N<sup>6</sup>-Dibenzyl-3,5-dimethyl-1,4-dithiine-2,6-dicarboxamide (S5)* A round bottom flask containing benzylamine (103 μL, 0.948 mmol, 2.2 equiv.) and triethylamine (0.15 mL, 1.08 mmol, 2.5 equiv.) in CH<sub>2</sub>Cl<sub>2</sub> (10 mL) was cooled to 0 °C. In a separate flask, diacyl chloride **9** that was freshly prepared from diacid **8** (100 mg, 0.431 mmol, 1.0 equiv.) according to the general procedure and was dissolved in CH<sub>2</sub>Cl<sub>2</sub> (10 mL) and added dropwise to the solution of benzylamine. After the addition was complete, the reaction was allowed to come to room temperature and stir overnight. The solution was poured into 1 M HCl (20 mL), and the layers were separated. The aqueous layer was further extracted with CH<sub>2</sub>Cl<sub>2</sub> (2 x 20 mL), and the organic layers were combined, washed with brine, dried over Na<sub>2</sub>SO<sub>4</sub>, filtered, and concentrated under reduced pressure to give an orange residue, which was purified by flash chromatography (0 → 8% MeOH in CH<sub>2</sub>Cl<sub>2</sub>) to give the title compound as an off-white solid (164 mg, 0.40 mmol, 93%). <sup>1</sup>H NMR (500 MHz, DMSO-*d*<sub>6</sub>) δ 8.82 (t, *J* = 6.1 Hz, 1H), 7.40 – 7.21 (m, 5H), 4.35 (d, *J* = 6.0 Hz, 2H), 2.20 (s, 3H). <sup>13</sup>C{<sup>1</sup>H} NMR (126 MHz, DMSO-*d*<sub>6</sub>) δ 163.2, 140.1, 128.3, 127.2, 126.9, 124.9, 42.6, 21.4. HRMS (Q-TOF-ESI-MS) *m/z*: [M+H]<sup>+</sup> Calcd for C<sub>22</sub>H<sub>23</sub>N<sub>2</sub>O<sub>2</sub>S<sub>2</sub><sup>+</sup> 411.1195; Found 411.1195.

## ASSOCIATED CONTENT

### Supporting Information.

The Supporting Information is available free of charge on the ACS Publications website at DOI: [insert]

Synthesis of starting materials, binding characterization,

electrochemical characterization, computational studies, NMR spectra (PDF)

Coordinates from computational studies (PDF)

Crystallographic data for Receptor **3** in CIF format (CIF)

## AUTHOR INFORMATION

### Corresponding Author

\*tswager@mit.edu

### Notes

The authors declare no competing financial interests.

## ACKNOWLEDGMENT

This work was supported by the U.S. Army Engineer Research and Development Center Environmental Quality Technology Program under contract W912HZ-17-2-0027 and the National Science Foundation through the Division of Chemistry (2004005). We are also grateful to the Camille and Henry Dreyfus Foundation for supporting D. Vander Griend as a Henry Dreyfus Teacher-Scholar. We would like to thank Dr. B. Qiao and Dr. N. A. Romero for insightful comments and discussions.

## REFERENCES

- Fried, S.; Mackie, B.; Nothwehr, E. Nitrate and Phosphate Levels Positively Affect the Growth of Algae Species Found in Perry Pond. *Tillers* **2003**, *4*, 21–24.
- Doney, S. C.; Fabry, V. J.; Feely, R. A.; Kleypas, J. A. Ocean Acidification: The Other CO<sub>2</sub> Problem. *Ann. Rev. Mar. Sci.* **2009**, *1*, 169–192.
- Smith, A. H.; Lingas, E. O.; Rahman, M. Contamination of Drinking Water by Arsenic in Bangladesh: A Public Health Emergency. *B. World. Health Organ.* **2000**, *78*, 1093–1103.
- Narukawa, T.; Inagaki, K.; Kuroiwa, T.; Chiba, K. The Extraction and Speciation of Arsenic in Rice Flour by HPLC-ICP-MS. *Talanta* **2008**, *77*, 427–432.
- Day, J. A.; Montes-Bayón, M.; Vonderheide, A. P.; Caruso, J. A. A Study of Method Robustness for Arsenic Speciation in Drinking Water Samples by Anion Exchange HPLC-ICP-MS. *Anal. Bioanal. Chem.* **2002**, *373*, 664–668.
- Sadiq Khan, S.; Riaz, M. Determination of UV Active Inorganic Anions in Potable and High Salinity Water by Ion Pair Reversed Phase Liquid Chromatography. *Talanta* **2014**, *122*, 209–213.
- Alahi, M. E. E.; Mukhopadhyay, S. C. Detection Methods of Nitrate in Water: A Review. *Sensor. Actuat. A-Phys.* **2018**, *280*, 210–221.
- Wang, D.-X.; Wang, M.-X. Anion- $\pi$  Interactions: Generality, Binding Strength, and Structure. *J. Am. Chem. Soc.* **2013**, *135*, 892–897.
- Wu, F.-Y.; Li, Z.; Wen, Z.-C.; Zhou, N.; Zhao, Y.-F.; Jiang, Y.-B. A Novel Thiourea-Based Dual Fluorescent Anion Receptor with a Rigid Hydrazine Spacer. *Org. Lett.* **2002**, *4*, 3203–3205.
- Hiscock, J. R.; Caltagirone, C.; Light, M. E.; Hursthouse, M. B.; Gale, P. A. Fluorescent Carbazolylurea Anion Receptors. *Org. Biomol. Chem.* **2009**, *7*, 1781–1783.
- Bao, X.; Wu, X.; Berry, S. N.; Howe, E. N. W.; Chang, Y.-T.; Gale, P. A. Fluorescent Squaramides as Anion Receptors and Transmembrane Anion Transporters. *Chem. Commun.* **2018**, *54*, 1363–1366.
- Rostami, A.; Colin, A.; Li, X. Y.; Chudzinski, M. G.; Lough, A. J.; Taylor, M. S. N, N' -Diarylsquaramides: General, High-Yielding Synthesis and Applications in Colorimetric Anion Sensing. *J. Org. Chem.* **2010**, *75*, 3983–3992.
- Tuo, D.-H.; Ao, Y.-F.; Wang, Q.-Q.; Wang, D.-X. Benzene Triimide Cage as a Selective Container of Azide. *Org. Lett.* **2019**, *21*, 7158–7162.
- Martínez-Mañez, R.; Sancenón, F. Fluorogenic and Chromogenic Chemosensors and Reagents for Anions. *Chem. Rev.* **2003**, *103*, 4419–4476.
- Zhao, Y.; Markopoulos, G.; Swager, T. M. <sup>19</sup>F NMR Fingerprints: Identification of Neutral Organic Compounds in a Molecular Container. *J. Am. Chem. Soc.* **2014**, *136*, 10683–10690.
- Zhao, Y.; Swager, T. M. Simultaneous Chirality Sensing of Multiple Amines by <sup>19</sup>F NMR. *J. Am. Chem. Soc.* **2015**, *137*, 3221–3224.
- Zhao, Y.; Chen, L.; Swager, T. M. Simultaneous Identification of Neutral and Anionic Species in Complex Mixtures without Separation. *Angew. Chem. Int. Ed.* **2016**, *55*, 917–921.
- Perrone, B.; Springhetti, S.; Ramadori, F.; Rastrelli, F.; Mancin, F. “NMR Chemosensing” Using Monolayer-Protected Nanoparticles as Receptors. *J. Am. Chem. Soc.* **2013**, *135*, 11768–11771.
- Teichert, J. F.; Mazunin, D.; Bode, J. W. Chemical Sensing of Polyols with Shapeshifting Boronic Acids as a Self-Contained Sensor Array. *J. Am. Chem. Soc.* **2013**, *135*, 11314–11321.
- Choi, S.-J.; Yoon, B.; Ray, J. D.; Netchaev, A.; Moores, L. C.; Swager, T. M. Chemiresistors for the Real-Time Wireless Detection of Anions. *Adv. Funct. Mater.* **2020**, *30*, 1907087.
- Liu, Y.; Qin, Y.; Jiang, D. Squaramide-Based Tripodal Ionophores for Potentiometric Sulfate-Selective Sensors with High Selectivity. *Analyst* **2015**, *140*, 5317–5323.
- Zahran, E. M.; Hua, Y.; Li, Y.; Flood, A. H.; Bachas, L. G. Triazolophanes: A New Class of Halide-Selective Ionophores for Potentiometric Sensors. *Anal. Chem.* **2010**, *82*, 368–375.
- Hein, R.; Borissov, A.; Smith, M. D.; Beer, P. D.; Davis, J. J. A Halogen-Bonding Foldamer Molecular Film for Selective Reagentless Anion Sensing in Water. *Chem. Commun.* **2019**, *55*, 4849–4852.
- Bayly, S. R.; Gray, T. M.; Chmielewski, M. J.; Davis, J. J.; Beer, P. D. Anion Templated Surface Assembly of a Redox-Active Sensory Rotaxane. *Chem. Commun.* **2007**, *2*, 2234–2236.
- Hein, R.; Beer, P. D.; Davis, J. J. Electrochemical Anion Sensing: Supramolecular Approaches. *Chem. Rev.* **2020**, *120*, 1888–1935.
- Evans, N. H.; Serpell, C. J.; Beer, P. D. A Redox-Active [3]Rotaxane Capable of Binding and Electrochemically Sensing Chloride and Sulfate Anions. *Chem. Commun.* **2011**, *47*, 8775–8777.
- Cao, Q.-Y.; Pradhan, T.; Kim, S.; Kim, J. S. Ferrocene-Appended Aryl Triazole for Electrochemical Recognition of Phosphate Ions. *Org. Lett.* **2011**, *13*, 4386–4389.
- Willener, Y.; Joly, K. M.; Moody, C. J.; Tucker, J. H. R. An Exploration of Ferrocenyl Ureas as Enantioselective Electrochemical Sensors for Chiral Carboxylate Anions. *J. Org. Chem.* **2008**, *73*, 1225–1233.
- Clare, J. P.; Statnikov, A.; Lynch, V.; Sargent, A. L.; Sibert, J. W. “Wurster-Type” Ureas as Redox-Active Receptors for Anions. *J. Org. Chem.* **2009**, *74*, 6637–6646.
- Zubi, A.; Wragg, A.; Turega, S.; Adams, H.; Costa, P. J.; Félix, V.; Thomas, J. A. Modulating the Electron-Transfer Properties of a Mixed-Valence System through Host-Guest Chemistry. *Chem. Sci.* **2015**, *6*, 1334–1340.
- Beer, P. D.; Gale, P. A.; Chen, G. Z. Mechanisms of Electrochemical Recognition of Cations, Anions and Neutral Guest Species by Redox-Active Receptor Molecules. *Coord. Chem. Rev.* **1999**, *185–186*, 3–36.
- Robinson, S. W.; Mustoe, C. L.; White, N. G.; Brown, A.; Thompson, A. L.; Kennepohl, P.; Beer, P. D. Evidence for

- Halogen Bond Covalency in Acyclic and Interlocked Halogen-Bonding Receptor Anion Recognition. *J. Am. Chem. Soc.* **2015**, *137*, 499–507.
33. Mullaney, B. R.; Partridge, B. E.; Beer, P. D. A Halogen-Bonding Bis-Triazolium Rotaxane for Halide-Selective Anion Recognition. *Chem. Eur. J.* **2015**, *21*, 1660–1665.
34. Sheetz, E. G.; Qiao, B.; Pink, M.; Flood, A. H. Programmed Negative Allostery with Guest-Selected Rotamers Control Anion-Anion Complexes of Stackable Macrocycles. *J. Am. Chem. Soc.* **2018**, *140*, 7773–7777.
35. Destecroix, H.; Renney, C. M.; Mooibroek, T. J.; Carter, T. S.; Stewart, P. F. N.; Crump, M. P.; Davis, A. P. Affinity Enhancement by Dendritic Side Chains in Synthetic Carbohydrate Receptors. *Angew. Chem. Int. Ed.* **2015**, *54*, 2057–2061.
36. Valkenier, H.; Judd, L. W.; Li, H.; Hussain, S.; Sheppard, D. N.; Davis, A. P. Preorganized Bis-Thioureas as Powerful Anion Carriers: Chloride Transport by Single Molecules in Large Unilamellar Vesicles. *J. Am. Chem. Soc.* **2014**, *136*, 12507–12512.
37. McNally, B. A.; Koulov, A. V.; Lambert, T. N.; Smith, B. D.; Joos, J.-B.; Sisson, A. L.; Clare, J. P.; Sgarlata, V.; Judd, L. W.; Magro, G.; Davis, A. P. Structure-Activity Relationships in Cholapod Anion Carriers: Enhanced Transmembrane Chloride Transport through Substituent Tuning. *Chem. Eur. J.* **2008**, *14*, 9599–9606.
38. Edwards, S. J.; Valkenier, H.; Busschaert, N.; Gale, P. A.; Davis, A. P. High-Affinity Anion Binding by Steroidal Squaramide Receptors. *Angew. Chem. Int. Ed.* **2015**, *54*, 4592–4596.
39. Leung, A. N.; Degenhardt, D. A.; Bühlmann, P. Effect of Spacer Geometry on Oxoanion Binding by Bis- and Tetrakis-Thiourea Hosts. *Tetrahedron* **2008**, *64*, 2530–2536.
40. Wang, M.-X.; Yang, H.-B. A General and High Yielding Fragment Coupling Synthesis of Heteroatom-Bridged Calixarenes and the Unprecedented Examples of Calixarene Cavity Fine-Tuned by Bridging Heteroatoms. *J. Am. Chem. Soc.* **2004**, *126*, 15412–15422.
41. Wang, D.-X.; Zheng, Q.-Y.; Wang, Q.-Q.; Wang, M.-X. Halide Recognition by Tetraoxacalix[2]Arene[2]Triazine Receptors: Concurrent Noncovalent Halide- $\pi$  and Lone-Pair- $\pi$  Interactions in Host-Halide-Water Ternary Complexes. *Angew. Chem. Int. Ed.* **2008**, *47*, 7485–7488.
42. Kobayashi, K.; Gajurel, C. L. The Chemistry of 1,4-Dithiins. *Sulf. Rep.* **1986**, *7*, 123–148.
43. Bisson, A. P.; Lynch, V. M.; Monahan, M.-K. C.; Anslyn, E. V. Recognition of Anions through NH- $\pi$  Hydrogen Bonds in a Bicyclic Cyclophane—Selectivity for Nitrate. *Angew. Chem. Int. Ed.* **1997**, *36*, 2340–2342.
44. Oh, J. H.; Kim, J. H.; Kim, D. S.; Han, H. J.; Lynch, V. M.; Sessler, J. L.; Kim, S. K. Synthesis and Anion Recognition Features of a Molecular Cage Containing Both Hydrogen Bond Donors and Acceptors. *Org. Lett.* **2019**, *21*, 4336–4339.
45. Gompper, R.; Euchner, H.; Kast, H. Umsetzungen  $\alpha,\beta$ -Ungesättigter  $\beta$ -Amino- und  $\beta$ -Hydroxy-Carbonylverbindungen mit Dischwefeldichlorid und Verwandten Verbindungen. *Justus Liebigs Ann. Chem.* **1964**, *675*, 151–174.
46. Merschky, M.; Schmuck, C. Synthesis and Kinetic Studies of a Low-Molecular Weight Organocatalyst for Phosphate Hydrolysis in Water. *Org. Biomol. Chem.* **2009**, *7*, 4895–4903.
47. SIVVU. <http://sivvu.org> (accessed May 1, 2020).
48. Vander Griend, D. A.; Bediako, D. K.; DeVries, M. J.; DeJong, N. A.; Heeringa, L. P. Detailed Spectroscopic, Thermodynamic, and Kinetic Characterization of Nickel(II) Complexes with 2,2'-Bipyridine and 1,10-Phenanthroline Attained via Equilibrium-Restricted Factor Analysis. *Inorg. Chem.* **2008**, *47*, 656–662.
49. Kazmierczak, N.; Chew, J. A.; Vander Griend, D. A. Bootstrap Methods for Estimating the Uncertainty of Binding Constants in the Hard-Modeling of Spectrophotometric Titration Data. *J. Chemometrics*, **2020**, submitted.
50. Barlow, R. Asymmetric Errors. In *PHYSTAT2003*, Menlo Park, CA, Sep 8–11, 2003; Lyons, L., Mount, R., Reitmeyer, R., Eds.; SLAC National Accelerator Laboratory: Menlo Park, CA, 2003; 250–255.
51. Parks, F. C.; Liu, Y.; Debnath, S.; Stutsman, S. R.; Raghavachari, K.; Flood, A. H. Allosteric Control of Photofoldamers for Selecting between Anion Regulation and Double-to-Single Helix Switching. *J. Am. Chem. Soc.* **2018**, *140*, 17711–17723.
52. Hibbert, D. B.; Thordarson, P. The Death of the Job Plot, Transparency, Open Science and Online Tools, Uncertainty Estimation Methods and Other Developments in Supramolecular Chemistry Data Analysis. *Chem. Commun.* **2016**, *52*, 12792–12805.
53. Thordarson, P. Determining Association Constants from Titration Experiments in Supramolecular Chemistry. *Chem. Soc. Rev.* **2011**, *40*, 1305–1323.
54. White, N. G. Antielectrostatically Hydrogen Bonded Anion Dimers: Counter-Intuitive, Common and Consistent. *CrystEngComm* **2019**, *21*, 4855–4858.
55. Weinhold, F.; Klein, R. A. Anti-Electrostatic Hydrogen Bonds. *Angew. Chem. Int. Ed.* **2014**, *53*, 11214–11217.
56. Fatila, E. M.; Twum, E. B.; Sengupta, A.; Pink, M.; Karty, J. A.; Raghavachari, K.; Flood, A. H. Anions Stabilize Each Other inside Macrocyclic Hosts. *Angew. Chem. Int. Ed.* **2016**, *55*, 14057–14062.
57. Zhao, W.; Qiao, B.; Chen, C.-H.; Flood, A. H. High-Fidelity Multistate Switching with Anion–Anion and Acid–Anion Dimers of Organophosphates in Cyanostar Complexes. *Angew. Chem. Int. Ed.* **2017**, *56*, 13083–13087.
58. He, Q.; Tu, P.; Sessler, J. L. Supramolecular Chemistry of Anionic Dimers, Trimers, Tetramers, and Clusters. *Chem* **2018**, *4*, 46–93.
59. Tawfik, D. S.; Viola, R. E. Arsenate Replacing Phosphate: Alternative Life Chemistries and Ion Promiscuity. *Biochemistry* **2011**, *50*, 1128–1134.
60. Ulatowski, F.; Dabrowa, K.; Bałakier, T.; Jurczak, J. Recognizing the Limited Applicability of Job Plots in Studying Host-Guest Interactions in Supramolecular Chemistry. *J. Org. Chem.* **2016**, *81*, 1746–1756.
61. Egdal, R. K.; Raber, G.; Bond, A. D.; Hussain, M.; Espino, M. P. B.; Francesconi, K. A.; McKenzie, C. J. Selective Recognition and Binding of Arsenate over Phosphate. *Dalton Trans.* **2009**, 9718–9721.
62. Elias, M.; Wellner, A.; Goldin-Azulay, K.; Chabriere, E.; Vorholt, J. A.; Erb, T. J.; Tawfik, D. S. The Molecular Basis of Phosphate Discrimination in Arsenate-Rich Environments. *Nature* **2012**, *491*, 134–137.
63. Dutta, R.; Bose, P.; Ghosh, P. Arsenate Recognition in Aqueous Media by a Simple Tripodal Urea. *Dalton Trans.* **2013**, *42*, 11371–11374.
64. Fatila, E. M.; Pink, M.; Twum, E. B.; Karty, J. A.; Flood, A. H. Phosphate-Phosphate Oligomerization Drives Higher Order Co-Assemblies with Stacks of Cyanostar Macrocycles. *Chem. Sci.* **2018**, *9*, 2863–2872.
65. Kempen, E. C.; Brodbelt, J. S. A Method for the Determination of Binding Constants by Electrospray Ionization Mass Spectrometry. *Anal. Chem.* **2000**, *72*, 5411–5416.
66. Richmond, T. G.; Johnson, J. R.; Edwards, J. O.; Rieger, P. H.

- Kinetics of Pyroarsenate Hydrolysis in Aqueous Solution. *Aust. J. Chem.* **1977**, *30*, 1187–1194.
67. Park, J. W.; Rhee, Y. M.; Kim, M. S. Can Adenosine Triarsenate Role as an Energy Carrier? *B. Korean Chem. Soc.* **2013**, *34*, 361–362.
68. Liu, Y.; Sengupta, A.; Raghavachari, K.; Flood, A. H. Anion Binding in Solution: Beyond the Electrostatic Regime. *Chem* **2017**, *3*, 411–427.
69. Dobscha, J. R.; Debnath, S.; Fadler, R. E.; Fatila, E. M.; Pink, M.; Raghavachari, K.; Flood, A. H. Host–Host Interactions Control Self-Assembly and Switching of Triple and Double Decker Stacks of Tricarbazole Macrocycles Co-Assembled with Anti-Electrostatic Bisulfate Dimers. *Chem. Eur. J.* **2018**, *24*, 9841–9852.
70. Amatore, C.; Azzabi, M.; Calas, P.; Jutand, A.; Lefrou, C.; Rollin, Y. Absolute Determination of Electron Consumption in Transient or Steady State Electrochemical Techniques. *J. Electroanal. Chem. Interf. Electrochem.* **1990**, *288*, 45–63.
71. Shine, H. J.; Silber, J. J.; Bussey, R. J.; Okuyama, T. Ion Radicals. XXV. The Reactions of Thianthrene and Phenothiazine Perchlorates with Nitrite Ion, Pyridine, and Other Nucleophiles. *J. Org. Chem.* **1972**, *37*, 2691–2697.
72. CYLview, 1.0b; Legault, C. Y., Université de Sherbrooke, 2009 (<http://www.Cylview.Org>).
73. Sather, A. C.; Berryman, O. B.; Rebek, J. Selective Recognition and Extraction of the Uranyl Ion. *J. Am. Chem. Soc.* **2010**, *132*, 13572–13574.
74. Latorre, A.; Lorca, R.; Zamora, F.; Somoza, Á. Enhanced Fluorescence of Silver Nanoclusters Stabilized with Branched Oligonucleotides. *Chem. Commun.* **2013**, *49*, 4950–4952.
75. Wallace, K. J.; Hanes, R.; Anslyn, E.; Morey, J.; Kilway, K. V.; Siegel, J. Preparation of 1,3,5-Tris(Aminomethyl)-2,4,6-Triethylbenzene from Two Versatile 1,3,5-Tri(Halosubstituted) 2,4,6-Triethylbenzene Derivatives. *Synthesis* **2005**, *2005*, 2080–2083.

## SYNOPSIS TOC (Word Style "SN\_Synopsis\_TOC").

